

# Evaluation of [ $^{11}\text{C}$ ]PipISB and [ $^{18}\text{F}$ ]PipISB in Monkey as Candidate Radioligands for Imaging Brain Cannabinoid Type-1 Receptors In Vivo

SJOERD J. FINNEMA,<sup>1</sup> SEAN R. DONOHUE,<sup>1,2</sup> SAMI S. ZOGHBI,<sup>2</sup> AMIRA K. BROWN,<sup>2</sup> BALÁZS GULYÁS,<sup>1</sup> ROBERT B. INNIS,<sup>2</sup> CHRISTER HALLDIN,<sup>1</sup> AND VICTOR W. PIKE<sup>2\*</sup>

<sup>1</sup>Karolinska Institutet, Department of Clinical Neuroscience, Psychiatry Section, Karolinska Hospital, S-17176 Stockholm, Sweden

<sup>2</sup>Molecular Imaging Branch, National Institute of Mental Health, National Institutes of Health, Bethesda, Maryland 20892

**KEY WORDS** positron emission tomography; carbon-11; fluorine-18; radiotracer

**ABSTRACT** *N*-(4-Fluorobenzyl)-4-[3-(piperidin-1-yl)indole-1-sulfonyl]benzamide (PipISB, **3**) is a selective and high-potency cannabinoid subtype-1 (CB<sub>1</sub>) receptor inverse agonist. We have previously reported radiosyntheses of [ $^{11}\text{C}$ ]**3** and [ $^{18}\text{F}$ ]**3**. Here, we aimed to evaluate the uptake and CB<sub>1</sub> receptor-specific binding of each radioligand in monkey brain in vivo with positron emission tomography (PET). [ $^{11}\text{C}$ ]**3** or [ $^{18}\text{F}$ ]**3** was injected intravenously into rhesus or cynomolgus monkey, respectively, and examined with PET at baseline or after pretreatment with a receptor-saturating dose of CB<sub>1</sub> receptor-selective ligand (**3** for [ $^{11}\text{C}$ ]**3** or **8** for [ $^{18}\text{F}$ ]**3**). In one PET experiment, the dose of **3** was administered at 100 min after [ $^{11}\text{C}$ ]**3**. Relative plasma concentrations of radioligand and radiometabolites were concurrently measured in baseline experiments with high-performance liquid chromatography. Brain radioactivity uptake was highest in striatum and cerebellum, and it reached 170–270% standardized uptake value (SUV) at 120 min after injection of [ $^{11}\text{C}$ ]**3** and 180% SUV at 240 min after injection of [ $^{18}\text{F}$ ]**3**. Radioactivity was well retained in all CB<sub>1</sub> receptor-rich regions. No reference region could be identified for nonspecifically bound radioligand. Under CB<sub>1</sub> receptor pretreatment and displacement conditions, initial brain uptakes of radioactivity were similar to those at baseline. Regional brain radioactivity concentrations then became homogeneous and diminished to between 70 and 80% SUV at 120 min after injection of [ $^{11}\text{C}$ ]**3** and to 25% SUV at 240 min after injection of [ $^{18}\text{F}$ ]**3**. [ $^{18}\text{F}$ ]**3** was not defluorinated but was metabolized to less lipophilic radiometabolites, as was [ $^{11}\text{C}$ ]**3**. Hence, [ $^{11}\text{C}$ ]**3** and [ $^{18}\text{F}$ ]**3** showed high CB<sub>1</sub> receptor-specific binding in monkey brain in vivo and merit further investigation as prospective PET radioligands in humans. *Synapse* 63:22–30, 2009. Published 2008 Wiley-Liss, Inc.<sup>†</sup>

## INTRODUCTION

*Cannabis sativa* (marijuana) intake has long been known to elicit alterations in cognition, pain sensation, and appetite. These effects are now attributed to modulation of a specific receptor class, the cannabinoid receptors (i.e., CB<sub>1</sub> and CB<sub>2</sub>) (Devane et al., 1988; Munro et al., 1993). Both CB<sub>1</sub> and CB<sub>2</sub> receptors are G-protein coupled and are the targets of several endogenous ligands (e.g., arachidonyl ethanolamide and 2-arachidonyl glycerol) (Devane et al., 1992; Mechoulam et al., 1995; Sugiura et al., 1995). The CB<sub>1</sub> subtype is abundantly expressed throughout the

body with highest densities in brain (Glass et al., 1997; Herkenham et al., 1990, 1991), especially in hippocampus, cerebellum (molecular layer), and basal ganglia, suggesting roles in memory storage, coordi-

Contract grant sponsor: National Institute of Mental Health; Contract grant number: Z01-MH-002795

\*Correspondence to: Victor W. Pike, Molecular Imaging Branch, National Institute of Mental Health, National Institutes of Health, Building 10, Rm B3 C346A, 10 Center Drive, Bethesda, MD 20892-1003, USA. E-mail: pikev@mail.nih.gov

Received 12 April 2008; Accepted 3 June 2008

DOI 10.1002/syn.20578

Published online in Wiley InterScience (www.interscience.wiley.com).

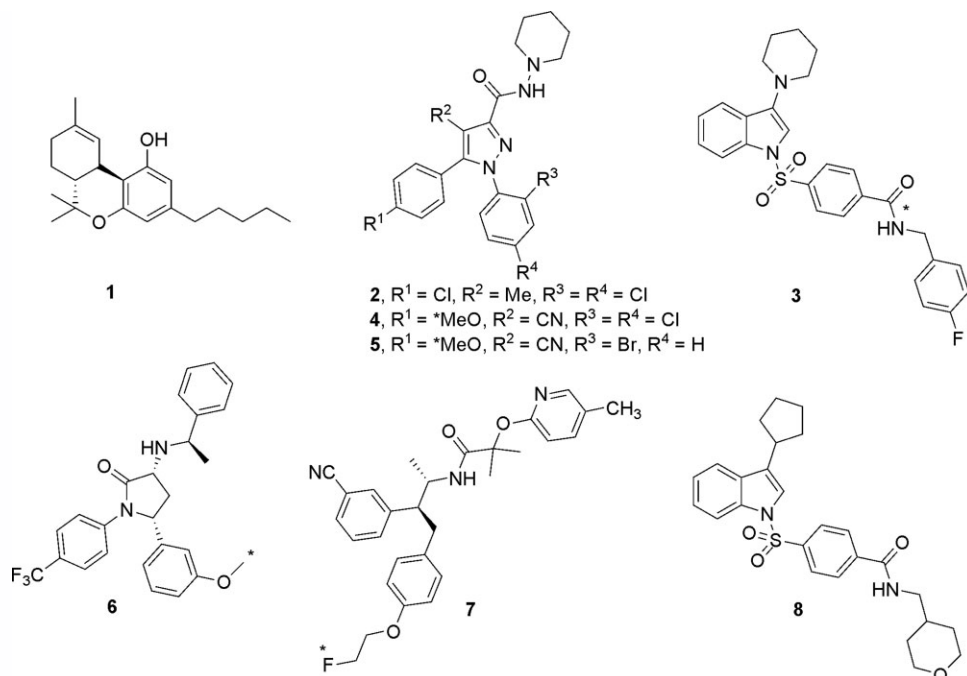


Fig. 1. Structures of  $\Delta^9$ -THC (**1**), SR 141716A (**2**), PipISB (**3**), JHU75528 (**4**), JHU75575 (**5**), MePPEP (**6**), MK-9470 (**7**), and ISPB (**8**). Asterisks denote sites of labeling with carbon-11 or fluorine-18.

nation, movement, thermal regulation, and appetite. CB<sub>2</sub> receptors are also in brain but are at their highest densities in the periphery where they interact with the immune system (Gong et al., 2006; Lynn and Herkenham, 1994; Munro et al., 1993).

Pharmacological modulation of CB<sub>1</sub> receptors is efficacious for treating several disorders. Exogenous CB<sub>1</sub> receptor agonists, such as  $\Delta^9$ -THC (dronabinol, **1**, Fig. 1) attenuate nausea and vomiting in chemotherapy (Darmani and Crim, 2005; Izzo and Coutts, 2005), stimulate appetite in wasting syndrome (Beal et al., 1995, 1997), and reduce muscle spasms in multiple sclerosis (Grundy, 2002; Pryce et al., 2003). Nevertheless, the medical uses of CB<sub>1</sub> receptor agonists are controversial because of the low benefit-risk margin and associated psychotropic response. Conversely, CB<sub>1</sub> receptor antagonists are now of major therapeutic interest. Some compounds formerly considered to be antagonists are currently considered to be inverse agonists as they inhibit intrinsic or spontaneous receptor signaling in cell systems expressing CB<sub>1</sub> receptors (Bouaboula et al., 1997; Landsman et al., 1997; Meschler et al., 2000). One of these inverse agonists, rimonabant (**2**, Fig. 1) (Rinaldi-Carmona et al., 1994), has been shown to improve therapeutic outcome in the treatment of metabolic disorders (Antel et al., 2006; Halford, 2006) and smoking addiction (Heningfield et al., 2005).

Molecular imaging of brain neuroreceptor systems in living subjects can play a significant role in clinical

research on neuropsychiatric conditions and also in drug discovery and development. Thus, positron emission tomography (PET) in tandem with an effective positron-emitting radioligand may be used to measure the changes in brain receptor densities in vivo in various disorders (Halldin et al., 2001) and also to perform drug receptor occupancy studies, which are of value in drug development preceding clinical trials (Mozley, 2005). So far, only a few PET radioligands have shown promise for imaging brain CB<sub>1</sub> receptors in vivo. These include inverse agonists from the 1,5-diarylpyrazole platform of rimonabant [e.g., [<sup>11</sup>C]JHU 75528 (<sup>11</sup>C]**4**, Fig. 1) (Fan et al., 2006; Horti et al., 2006) and [<sup>11</sup>C]JHU 75575 (<sup>11</sup>C]**5**, Fig. 1) (Fan et al., 2006)] and from two other structurally distinct platforms [i.e., [<sup>11</sup>C]MePPEP (<sup>11</sup>C]**6**, Fig. 1) (Yasuno et al., 2008) and [<sup>18</sup>F]MK-9470 (<sup>18</sup>F]**7**, Fig. 1) (Burns et al., 2007; Liu et al., 2007)].

PipISB [*N*-(4-fluorobenzyl)-4-[3-(piperidin-1-yl)indole-1-sulfonyl]benzamide] (**3**, Fig. 1) has favorable physical and pharmacological properties for development as a PET radioligand for brain CB<sub>1</sub> receptors (Allen et al., 2005; Donohue et al., 2008). These include lipophilicity (cLog<sub>D7.4</sub> = 5.14) similar to other promising radioligands, high potency (*K<sub>b</sub>* = 1.5 nM) and high selectivity versus the CB<sub>2</sub> receptor (*K<sub>b</sub>* = >7000 nM). We have previously reported the labeling of **3** with carbon-11 or fluorine-18 (Donohue et al., 2008). Here we evaluate the suitability of [<sup>11</sup>C]**3** and [<sup>18</sup>F]**3** as brain CB<sub>1</sub> receptor PET radioligands in monkey.

## MATERIALS AND METHODS

### Radioligands

[<sup>11</sup>C]**3** and [<sup>18</sup>F]**3** were synthesized in high radiochemical purity (>98%), as described previously (Donohue et al., 2008). Briefly, [<sup>11</sup>C]**3** was prepared with a modified Synthia apparatus (Bjurling et al., 1995) in one step from [<sup>11</sup>C]carbon monoxide (itself prepared from cyclotron-produced [<sup>11</sup>C]carbon dioxide). The label was introduced into the carbonyl position. [<sup>18</sup>F]**3** was prepared in a two-stage, four-step synthesis from cyclotron-produced [<sup>18</sup>F]fluoride ion using [<sup>18</sup>F]4-fluorobenzyl bromide as the key labeling agent in a custom-made remotely controlled apparatus.

### PET measurements in monkeys

#### Rhesus monkey

Experiments in male rhesus monkey (*Macaca mulatta*) were performed at the National Institute of Mental Health (NIMH) according to the “Guide for the Care and Use of Laboratory Animals” (Clark et al., 1996) and were approved by the Animal Care and Use Committee. Two male rhesus monkeys were studied. The monkeys were immobilized with ketamine (10 mg/kg, i.m.) before imaging and, at the PET suite, intubated and placed under isoflurane anesthesia (1–2%). Scans were started at least 90 min after ketamine administration. Radioactivity in brain was measured with an Advance tomograph (GE Medical Systems, Milwaukee, WI). This camera has effective transaxial and axial field-of-views of 55 and 15 cm, respectively. A total of four PET experiments were conducted. One monkey (A, weight 10 kg) was studied in one day on which a baseline experiment was followed by a pretreatment experiment. The second monkey (B, weight 16 kg) was evaluated on one day for a baseline experiment and on another for a displacement experiment. For all experiments, radioligand was administered by bolus injection over ~30 s. Scans of 120 min (33 frames) were acquired in all studies, except for the displacement study (180 min, 45 frames).

For Monkey A at baseline, [<sup>11</sup>C]**3** (191 MBq) was injected with a specific radioactivity of 72 GBq/μmol resulting in an associated mass of carrier **3** of 1.3 μg (2.65 nmol; 0.27 nmol/kg). For the pretreatment experiment, **3** (1.0 mg/kg, i.v.) was infused at 20 min before [<sup>11</sup>C]**3** (180 MBq; 23 GBq/μmol; mass of **3**: 3.8 μg, 7.77 nmol; 0.78 nmol/kg). Monkey B at baseline was injected with [<sup>11</sup>C]**3** (141 MBq; 31 GBq/μmol; mass of **3**: 2.2 μg, 4.55 nmol; 0.28 nmol/kg). For the displacement experiment, **3** (1.5 mg/kg, i.v.) was infused over a 2-min period at 100 min after injection of [<sup>11</sup>C]**3** (283 MBq; 32 GBq/μmol; mass of **3**: 4.3 μg, 8.84 nmol; 0.55 nmol/kg).

#### Cynomolgus monkey

Cynomolgus monkey (*Macaca fascicularis*) experiments were performed at the Karolinska Institutet (KI) according to the “Guidelines for planning, conducting and documenting experimental research” (Dnr 4820/06-600) of the KI as well as the “Guide for the Care and Use of Laboratory Animals” (Clark et al., 1996). The study was approved by the Animal Ethics Committee of the Swedish Animal Welfare Agency. One female cynomolgus monkey (weight 4.9 kg) was studied in the two PET experiments. Anesthesia was induced and maintained with repeated i.m. injections of a mixture of ketamine hydrochloride [3.75 mg/(kg h) Ketalar<sup>®</sup>, Pfizer] and xylazine hydrochloride [1.5 mg/(kg h) Rompun<sup>®</sup> Vet., Bayer]. Radioactivity in brain was measured with an ECAT EXACT HR system (Siemens, Knoxville, TN). This camera has a patient port and axial field-of-view of 56 and 15 cm, respectively (Wienhard et al., 1994). For both experiments, the radioligand was injected intravenously as a bolus over ~5 s. Scans (34 frames) were acquired over 240 min in both experiments.

Under the baseline condition, the injected [<sup>18</sup>F]**3** (49 MBq) had a specific radioactivity of 261 GBq/μmol and an injected mass of **3** of 0.1 μg (0.19 nmol; 0.039 nmol/kg). In the pretreatment experiment, the CB<sub>1</sub>-selective ligand, 4-(3-cyclopentyl-indole-1-sulfonyl)-N-(tetrahydro-pyran-4-yl-methyl)-benzamide (ISPB; **8**, 1.0 mg/kg, i.v., Fig. 1) (Allen et al., 2005; Yasuno et al., 2008), was infused over a 1-min period (15 min before radioligand injection) to block CB<sub>1</sub> receptors. The injected [<sup>18</sup>F]**3** (55 MBq) had a specific radioactivity of 229 GBq/μmol and an injected mass of **3** of 0.12 μg (0.24 nmol; 0.049 nmol/kg).

### Image analysis

#### Rhesus monkey

The mean image of the baseline PET measurement (10–120 min) was coregistered and resliced to a resampled MRI (0.78, 0.78, and 1.5 mm) in PMOD (Version 2.65, Zurich, Switzerland). Generated transformation parameters were concurrently applied to all frames of the corresponding baseline and pretreatment study. For the displacement study in Monkey B, the mean image from 10 to 100 min was used. Volumes of interest (VOIs) were manually defined on the coronal planes of the MRI. Similar VOIs were applied, as reported by Yasuno et al. (2008), including cerebellum (2.2 and 2.1 cm<sup>3</sup>), frontal cortex (9.2 and 7.8 cm<sup>3</sup>), lateral temporal cortex (4.7 and 4.5 cm<sup>3</sup>), medial temporal cortex (3.3 and 3.0 cm<sup>3</sup>), striatum (1.5 and 2.1 cm<sup>3</sup>), thalamus (0.8 and 0.6 cm<sup>3</sup>), and pons (0.7 and 0.6 cm<sup>3</sup>) (values are for Monkeys A and B, respectively).

Tissue radioactivity concentrations were decay-corrected to normalize for injected dose and body weight,

expressed as % standardized uptake values (%SUV), where

$$\% \text{SUV} = \frac{\% \text{ Injected activity}}{\text{Brain tissue (g)}} \times \text{Body weight (g)}$$

### Cynomolgus monkey

The mean image of the PET measurements (8–240 min) was transformed into a standard anatomical space using the monkey version of the Human Brain Atlas developed at the Karolinska Institutet (Roland et al., 1994). The transformation matrix generated on this image was applied to all frames of the corresponding baseline and pretreatment experiments. PET data were subsequently resliced to a similar resolution as for the rhesus monkeys (1.00, 1.00, 1.00 mm). VOIs were manually defined on the coronal planes of an average monkey MRI. Comparable VOIs were applied as for the rhesus monkeys, including cerebellum (1.9 cm<sup>3</sup>), frontal cortex (7.4 cm<sup>3</sup>), lateral temporal cortex (5.0 cm<sup>3</sup>), medial temporal cortex (2.9 cm<sup>3</sup>), striatum (2.1 cm<sup>3</sup>), thalamus (0.9 cm<sup>3</sup>), and pons (0.7 cm<sup>3</sup>). Tissue radioactivity concentrations were expressed as %SUV, as described for rhesus monkeys.

#### Measurement of radioligand and radiometabolites in plasma

The stability of **3** in formulation vehicle (over 30 min) and in plasma in vitro over 30 min was assessed using  $[^{11}\text{C}]\mathbf{3}$  and HPLC analysis (Zoghbi et al., 2006). The distribution of **3** between plasma and cells was measured using  $[^{11}\text{C}]\mathbf{3}$ , with the method described previously (Zoghbi et al., 2006).

Before analyses of  $[^{11}\text{C}]\mathbf{3}$  and its radiometabolites in rhesus monkey plasma, the radiochemical purity of the radioligand was checked with HPLC. Arterial plasma samples (1 ml each) were continuously drawn from rhesus monkey at every 15 s for 2 min after injection of radioligand and followed by samples drawn at 3, 5, 10, 30, 60, 90, and 120 min. Plasma samples were analyzed for radioactivity composition with HPLC as described previously (Zoghbi et al., 2006), using a reverse phase column (Nova-Pak C18, 4  $\mu\text{m}$ , 100 mm  $\times$  8 mm; Waters Corp.) housed within a radial compression module (RCM-100), eluted at 2 ml/min with  $\text{MeOH-H}_2\text{O:Et}_3\text{N}$  (80:20:0.1 by volume).

The plasma-free fraction was determined using Amicon centrifree filters and ultracentrifugation as described previously (Gandelman et al., 1994).

For measurement of  $[^{18}\text{F}]\mathbf{3}$  and its radiometabolites in cynomolgus plasma, venous blood (2 ml) was sampled from monkey at 7, 33, 64, and 93 min after injection of radioligand. Plasma samples were analyzed as described

previously (Halldin et al., 1995), using a reverse phase column ( $\mu\text{-Bondapak C-18}$  column; 7.8 mm  $\times$  300 mm, 10  $\mu\text{m}$ ; Waters) eluted at 6 ml/min with a gradient of  $\text{MeCN}$  (A) and  $\text{aq-H}_3\text{PO}_4$  (0.01 M) (B), with A increasing linearly from 30% v/v at 0 min to 75% v/v at 4 min, then decreasing linearly to 30% v/v at 7.5 min and then held isocratic at 30% v/v over 2.5 min.

## RESULTS

### PET measurements in monkeys

#### Rhesus monkey

After intravenous injection of  $[^{11}\text{C}]\mathbf{3}$  into two rhesus monkeys, brain radioactivity reached 170% for Monkey A (Fig. 2, Panel A) and 270% SUV for Monkey B at 120 min after injection (data not shown). For both monkeys, brain radioactivity uptake was highest in striatum and cerebellum ( $\sim 170\%$  SUV), moderate in cortex and thalamus ( $\sim 140\%$  SUV), and lowest in pons ( $\sim 100\%$  SUV). Radioactivity slowly increased in all  $\text{CB}_1$  receptor-rich regions until the end of the scan (120 min). Under pretreatment conditions with **3** (1 mg/kg, i.v.), the initial 5-min uptake of radioactivity in the brain was similar to that in the baseline experiment of the same monkey (A), but thereafter the regional brain radioactivities diminished to 65% SUV (at 120 min after injection) (Fig. 2, Panel B). In the displacement experiment, with **3** (1.5 mg/kg, i.v.), initial uptake of radioactivity in the brain was again similar to that in the baseline experiment, but after displacement radioactivity in all brain regions decreased to 70–80% SUV (180 min after injection) (Fig. 2, Panel C).

#### Cynomolgus monkey

After i.v. injection of  $[^{18}\text{F}]\mathbf{3}$  into cynomolgus monkey, brain radioactivity reached 180% SUV at 240 min after injection (Fig. 3, Panel A). The regional distribution of radioactivity was similar to that seen for  $[^{11}\text{C}]\mathbf{3}$  and well retained to the end of the scan (240 min). In the same monkey pretreated with **8** (1 mg/kg, i.v.), regional brain radioactivities became similar and diminished to 25% SUV (240 min after injection) (Fig. 3, Panel B).

#### Summation images of $[^{11}\text{C}]\mathbf{3}$ and $[^{18}\text{F}]\mathbf{3}$

Figure 4 shows PET summation images at the level of the striatum in rhesus monkey brain acquired between 10 and 120 min with  $[^{11}\text{C}]\mathbf{3}$  (Panel A) and in cynomolgus monkey brain acquired between 8 and 240 min with  $[^{18}\text{F}]\mathbf{3}$  (Panel C). Radioactivity was distributed according to previously established  $\text{CB}_1$  receptor densities (Glass et al., 1997; Herkenham et al., 1990, 1991). The images from the corresponding pretreatment experiments showed a low radioactivity concentration across brain (Fig. 4, Panels B and D for  $[^{11}\text{C}]\mathbf{3}$  and  $[^{18}\text{F}]\mathbf{3}$ , respectively).

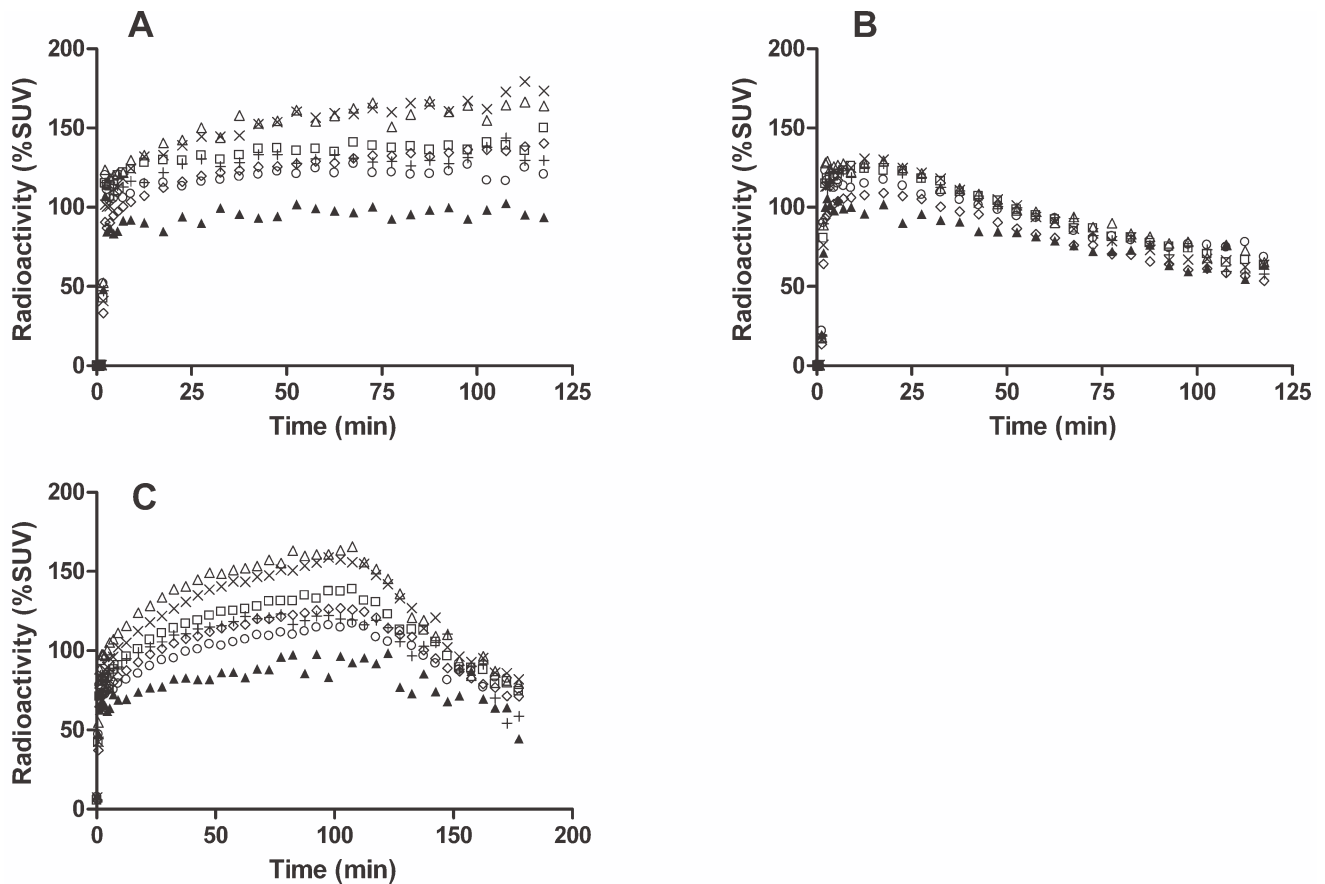


Fig. 2. Regional time-radioactivity curves in rhesus monkey brain after i.v. injection of [ $^{11}\text{C}$ ]3 in Monkey A (Panel A), after pretreatment of Monkey A with **3** (1 mg/kg, i.v.) (Panel B), and in Monkey B with **3** (1.5 mg/kg, i.v.) administered as a displacing agent at 100 min (Panel C). Key:  $\times$ , striatum;  $\triangle$ , cerebellum;  $\diamond$ , frontal cortex;  $\square$ , lateral temporal cortex;  $+$ , thalamus;  $\circ$ , medial temporal cortex;  $\blacktriangle$ , pons.

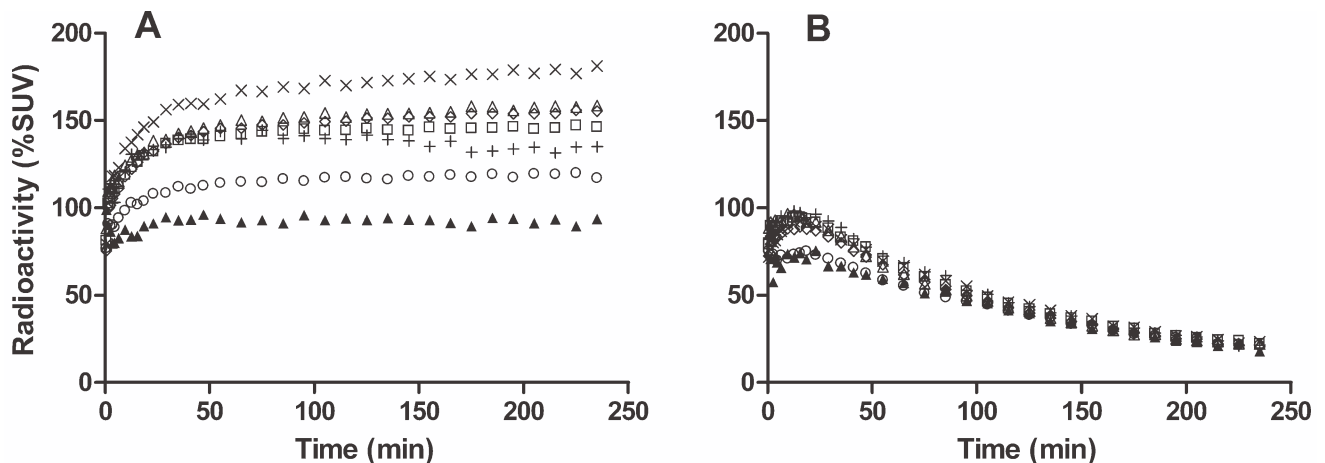


Fig. 3. Regional time-radioactivity curves in cynomolgus monkey brain after i.v. injection of [ $^{18}\text{F}$ ]3 (Panel A) and after pretreatment with **8** (1 mg/kg, i.v.) (Panel B). Key:  $\times$ , striatum;  $\triangle$ , cerebellum;  $\diamond$ , frontal cortex;  $\square$ , lateral temporal cortex;  $+$ , thalamus;  $\circ$ , medial temporal cortex;  $\blacktriangle$ , pons.

#### Measurement of radioligands and radiometabolites in plasma

Measurements with [ $^{11}\text{C}$ ]3 showed that **3** was stable (98.2% unchanged) in vitro and in whole blood for

30 min at room temperature and distributed 31 and 69% between cellular and plasma blood components, respectively. The free fraction of **3** in pooled human plasma was about 0.23%.

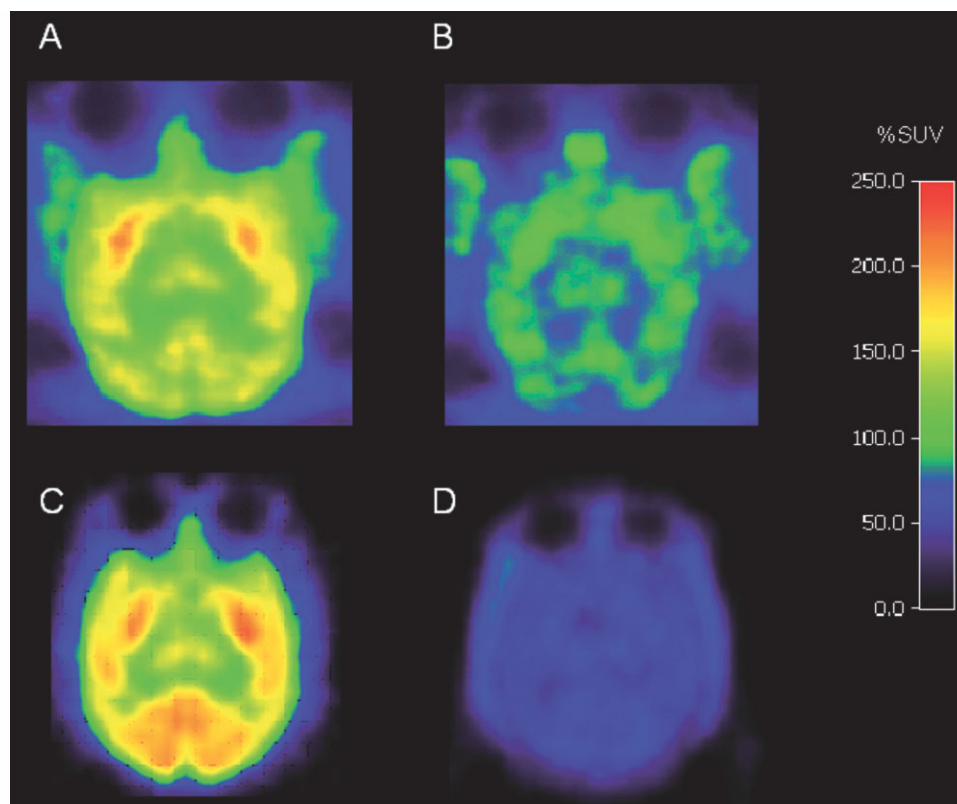


Fig. 4. Horizontal PET images obtained at the level of the striatum in monkey: mean of images acquired from 10 to 120 min after injection with [<sup>11</sup>C]**3** in rhesus Monkey A under baseline conditions (Panel A) and after pretreatment with **3** (1 mg/kg, i.v.) (Panel B); mean of images summed for data acquired between 8 and 240 min after injection of cynomolgus monkey with [<sup>18</sup>F]**3** under baseline conditions (Panel C) and after pretreatment with **8** (1 mg/kg, i.v.) (Panel D).

After i.v. injection of [<sup>11</sup>C]**3** into rhesus monkey at baseline, 20% of the radioactivity in plasma was unchanged radioligand at 60 min. This value remained similar until the end of the scan (120 min after injection) (Fig. 5, Panel B). Two radiometabolite fractions (RM<sub>1</sub> and RM<sub>2</sub>) with shorter reverse phase HPLC retention times ( $t_{RS} = 2.4$  and 3.8 min, respectively) than radioligand ( $t_R = 7.8$  min) were observed (Fig. 5, Panel A). At the end of the scan, these radiometabolites represented about 40% of the radioactivity in plasma, whereas the radioactivity that could not be extracted from plasma for analysis represented 31.9%.

After i.v. injection of [<sup>18</sup>F]**3** into cynomolgus monkey at baseline, radioligand decreased to 57% of radioactivity in plasma at 93 min (Fig. 6, Panel B). There were three radiometabolite fractions (CM<sub>1</sub>, CM<sub>2</sub>, and CM<sub>3</sub>) with shorter retention times ( $t_{RS} = 2.8$ , 4.5, and 5.4 min, respectively) than the radioligand ( $t_R = 6.5$  min) (Fig. 6, Panel A). CM<sub>1</sub>, CM<sub>2</sub>, and CM<sub>3</sub> slowly increased to 16, 15, and 12% of radioactivity in plasma at 90 min after injection.

## DISCUSSION

### PET measurements in monkeys

Injection of [<sup>11</sup>C]**3** into rhesus Monkey A under baseline conditions resulted in good brain uptake of

radioactivity with a discrete regional distribution (Fig. 2, Panel A). Radioactivity uptakes at 120 min were greatest in striatum and cerebellum, modest in cortex and thalamus, and lowest in pons (Fig. 2, Panel A). This distribution corresponds to that expected from the autoradiography of brain CB<sub>1</sub> receptors in rhesus monkey (Herkenham et al., 1990), and from PET studies of other CB<sub>1</sub> radioligands, such as [<sup>11</sup>C]MePPEP (Yasuno et al., 2008).

Despite the promising brain uptake, the baseline experiments revealed two problems with [<sup>11</sup>C]**3**. The first problem is common to all PET CB<sub>1</sub> receptor radioligands in monkey, the lack of a reference region for free and nonspecifically bound radioligand. The pons, a region with low CB<sub>1</sub> receptor density, could not serve as a reference region because of contamination of measurements with radioactivity from the nearby CB<sub>1</sub> receptor-rich cerebellum through the partial volume effect. The second problem was the continuing slow increase in radioactivity throughout the 2-h scan, which precluded estimation of the time of peak equilibrium. In this respect, these kinetics resemble those reported for the CB<sub>1</sub> receptor radioligand [<sup>18</sup>F]**7** in rhesus monkey (Burns et al., 2007). In the case of [<sup>18</sup>F]**7**, area under the curve (AUC) analy-

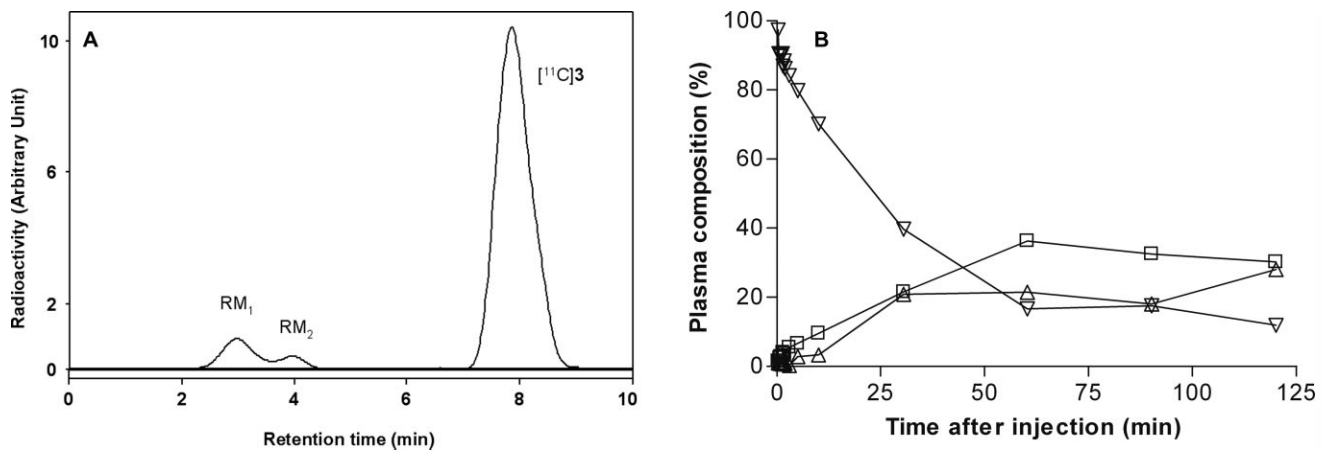


Fig. 5. HPLC of plasma at 10 min after i.v.  $[^{11}\text{C}]\mathbf{3}$  injection into rhesus monkey (Panel A) under baseline conditions. Corresponding time course of radioactivity in plasma (%) represented by parent radioligand and radiometabolite fractions (Panel B). Key:  $\nabla$ , parent radioligand,  $[^{11}\text{C}]\mathbf{3}$ ;  $\square$ , radiometabolite fraction,  $\text{RM}_1$ ;  $\triangle$ , radiometabolite fraction,  $\text{RM}_2$ .

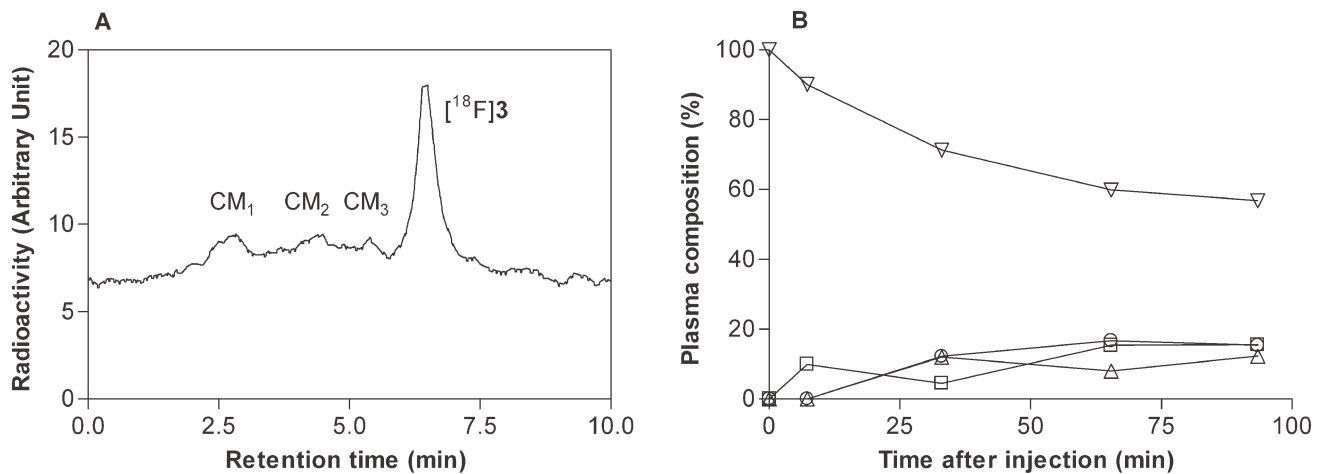


Fig. 6. HPLC of plasma at 60 min after injection of  $[^{18}\text{F}]\mathbf{3}$  into cynomolgus monkey under baseline conditions (Panel A). Corresponding time course of radioactivity in plasma (%) represented by parent radioligand and radiometabolite fractions after (Panel B). Please note that data is not corrected for radioactivity in blood pellet. Key:  $\nabla$ , parent radioligand,  $[^{18}\text{F}]\mathbf{3}$ ;  $\square$ , radiometabolite fraction,  $\text{CM}_1$ ;  $\circ$ , radiometabolite fraction,  $\text{CM}_2$ ;  $\triangle$ , radiometabolite fraction,  $\text{CM}_3$ .

sis proved to be suitable for estimating receptor availability (Burns et al., 2007), and therefore this approach might also prove applicable to  $[^{11}\text{C}]\mathbf{3}$ , but was not tested here.

When  $\text{CB}_1$  receptors were blocked with  $\mathbf{3}$  before the administration of  $[^{11}\text{C}]\mathbf{3}$ , the initial brain uptake of radioactivity was similar to that in the baseline experiment performed in the same monkey. This uptake was followed by steady washout of radioactivity from all regions down to a similar low level at the end of the scanning session (Fig. 2, Panel B). This experiment confirmed that  $[^{11}\text{C}]\mathbf{3}$  had bound specifically and reversibly to  $\text{CB}_1$  receptors in the baseline experiment. The ratios of regional radioactivity uptakes in the baseline experiment to those in the pretreatment experiment at 120 min provide crude estimates of the ratio of specific to nonspecific

binding; this value is about three for receptor-rich cerebellum.

In an experiment in the second monkey (B), administration of  $\mathbf{3}$  after  $[^{11}\text{C}]\mathbf{3}$  caused a rapid washout of a high proportion of radioactivity from all examined brain regions down to a common low level (Fig. 2, Panel C). This confirmed the presence of substantial receptor-specific binding and its reversibility. In this experiment, the magnitude of the early uptake and retention of radioactivity in all examined brain regions was similar to that seen for Monkey A at baseline. However, in a separate baseline experiment in Monkey B, the uptake of radioactivity was appreciably higher (270% SUV), although brain radioactivity kinetics were qualitatively similar. We have no explanation for this particular quantitative difference.

The finding that  $[^{11}\text{C}]\mathbf{3}$  ( $^{11}\text{C}$ ,  $t_{1/2} = 20.4$  min) gave slowly increasing radioactivity in brain warranted an investigation of longer-lived fluorine-18 ( $t_{1/2} = 109.7$  min) labeled  $\mathbf{3}$ , principally to extend the duration of scans in search of equilibrium binding. It was necessary to prepare  $[^{18}\text{F}]\mathbf{3}$  at a different center and, therefore, to use cynomolgus rather than rhesus monkeys in the PET experiments, and also to use different PET cameras and procedures (anesthesia, radiometabolite analysis). The use of different species of monkey probably had minimal effect since numerous studies have used either species in PET radioligand studies without gross differences in results. We used large regions of interest which would compensate for differences in brain size. Likewise, the use of different PET cameras was also probably without major effect as they have similar resolution and are each calibrated against an external standard.

After injection of  $[^{18}\text{F}]\mathbf{3}$  into cynomolgus monkey, the brain uptake and regional distribution of radioactivity (Fig. 3, Panel A) was similar to that of  $[^{11}\text{C}]\mathbf{3}$  in rhesus monkey (Fig. 2, Panels A and C). Despite the increase in available spatial resolution and scan time from fluorine-18, no reference region and no washout phase were observed. In the experiment in which  $\text{CB}_1$  receptors were selectively preblocked with ligand,  $\mathbf{8}$ , the initial brain uptake of radioactivity was similar to that in the baseline experiment, but thereafter rapidly and continuously decreased in all regions (Fig. 3, Panel B). The kinetics in this pretreatment experiment were very similar to those in the pretreatment experiment with  $[^{11}\text{C}]\mathbf{3}$  (Fig. 2, Panel B), despite the different species of monkey and different circumstances of data acquisition. The ratio of the concentration of brain radioactivity in receptor-rich cerebellum under baseline condition to that under the pretreatment condition was about 3 at 115 min after injection and therefore also quite similar to that obtained with  $[^{11}\text{C}]\mathbf{3}$ . Because  $[^{11}\text{C}]\mathbf{3}$  and  $[^{18}\text{F}]\mathbf{3}$  exhibited similar brain uptake and kinetics over the initial 125-min period after injection, the brain ingress of radiometabolites is probably not a major issue for either radioligand. The estimated ratio of specific binding (Fig. 3, Panel A) to nonspecific binding (Fig. 3, Panel B) in cerebellum increases to about 7 at 240 min after injection of  $[^{18}\text{F}]\mathbf{3}$ , implying over 80%  $\text{CB}_1$  receptor-specific binding in the baseline experiment. Images from the last frame of the experiment with  $[^{18}\text{F}]\mathbf{3}$  showed no skull uptake of radioactivity, thereby showing the absence of defluorination. Skull uptake of radioactivity would otherwise be troublesome for quantitation by causing errors in brain measurements through partial volume effects. Sharper images were obtained with  $[^{18}\text{F}]\mathbf{3}$  (Fig. 4, Panel C) than with  $[^{11}\text{C}]\mathbf{3}$  (Fig. 4, Panel A). Images from the pretreatment experiments (Fig. 4, Panels B and D) show the more complete washout of radioactivity for  $[^{18}\text{F}]\mathbf{3}$  because of the longer scan duration.

### Measurements of radioligands and radiometabolites in plasma

After baseline injection of  $[^{11}\text{C}]\mathbf{3}$  into rhesus monkey, two radiometabolites ( $\text{RM}_1$  and  $\text{RM}_2$ ) emerged quite rapidly in plasma (Fig. 5). By contrast, three radiometabolites ( $\text{CM}_1$ ,  $\text{CM}_2$ , and  $\text{CM}_3$ ) of  $[^{18}\text{F}]\mathbf{3}$  emerged slowly in cynomolgus monkey plasma (Fig. 6). The fact that the ratio of radioligand to radiometabolites in plasma at any given time depends on the radionuclide label may be due to the differences in the rates of clearance of different radiometabolite species from plasma, rather than to significant species differences in pattern of metabolism. All the radiometabolites had shorter retention times than parent radioligand [Figs. 5 (Panel A) and 6 (Panel A)], so indicating that they are less lipophilic than parent radioligand. Their abilities to pass the blood-brain barrier are unknown. Nevertheless, the striking similarity in the brain kinetics of the two radioligands suggests that neither is heavily contaminated with radiometabolites.

The plasma-free fraction of  $\mathbf{3}$  in pooled human blood is very low but still measurable with accuracy if required for biomathematical modeling of PET data.

### CONCLUSIONS

$[^{11}\text{C}]\mathbf{3}$  and  $[^{18}\text{F}]\mathbf{3}$  behaved as  $\text{CB}_1$  receptor-selective radioligands in vivo, with a high ratio of specific to nonspecific binding.  $[^{18}\text{F}]\mathbf{3}$  may have greater value for PET imaging because it shows no defluorination and permits a longer scan time. However, its radiosynthesis is multistage and lower yielding than that of  $[^{11}\text{C}]\mathbf{3}$ . These radioligands merit further investigation in human subjects where possible species differences in kinetics and metabolism may ultimately determine their utility with respect to other promising radioligands, such as  $[^{11}\text{C}]\text{MePPEP}$ .

### ACKNOWLEDGMENTS

This work was supported by the Intramural Program of the National Institute of Mental Health (project # Z01-MH-002795). Mr. S. R. Donohue was also supported with a studentship under the NIH-Karolinska Institutet Graduate Training Partnership in Neuroscience. The authors are grateful to Eli Lilly and Co. for the provision of compounds  $\mathbf{3}$  and  $\mathbf{8}$  under a CRADA (Cooperative Research and Development Agreement with NIMH), and to Dr. J. Schaus, Dr. L. Phebus, Mr. E. Chernet, and Mr. K. Ruley (Eli Lilly and Co) for useful discussions. The staff of the NIH Clinical PET Center is thanked for cyclotron production of carbon-11.

### REFERENCES

- Allen JB, Amegadzie AK, Gardinier KM, Gregory GS, Hitchcock SA, Hoogstraat PJ, Jones WJ, Jr, Smith DL. 2005. Preparation of arylsulfonyl-substituted indoles as  $\text{CB}_1$  receptor modulators. *PCT Int Appl WO 2005, 066,126*.

- Antel J, Gregory PC, Nordheim U, Nicholson JR, Dokladny K, Dunant P, Hofbauer KG, Szabo B, Niederhoffer N, Bock C. 2006. CB<sub>1</sub> cannabinoid receptor antagonists for treatment of obesity and prevention of comorbid metabolic disorders. *J Med Chem* 49:4008–4016.
- Beal JE, Olson R, Laubenstein L, Morales JO, Bellman P, Yangco B, Lefkowitz L, Plasse TF, Shepard KV. 1995. Dronabinol as a treatment for anorexia associated with weight loss in patients with AIDS. *J Pain Symptom Manage* 10:89–97.
- Beal JE, Olson R, Lefkowitz L, Laubenstein L, Bellman P, Yangco B, Morales JO, Murphy R, Powderly W, Plasse TF, Mosdell KW, Shepard KV. 1997. Long-term efficacy and safety of dronabinol for acquired immunodeficiency syndrome-associated anorexia. *J Pain Symptom Manage* 14:7–14.
- Bjurling P, Reineck R, Westerberg G, Schultz J, Gee AD, Sutcliffe J, Långström B. 1995. In Proceedings of the Vth Workshop on Targetry and Target Chemistry, Vancouver, BC, Canada. Link JM, Ruth TJ, editors. p 282–284. <http://trshare.triumf.ca/~buckley/wttc/pdf/1995/Sec7-20.pdf>
- Bouaboula M, Perrachon S, Milligan L, Canat X, Rinaldi-Carmona M, Portier M, Barth F, Calandras B, Pececu F, Lupker J, Maffrand J-P, Le Fur G, Casellas P. 1997. A selective inverse agonist for central cannabinoid receptor inhibits mitogen-activated protein kinase activation stimulated by insulin or insulin-like growth factor 1. Evidence for a new model of receptor/ligand interactions. *J Biol Chem* 272:22330–22339.
- Burns HD, Van Laere K, Sanabria-Bohorquez S, Hamill TG, Bormans G, Eng WS, Gibson R, Ryan C, Connolly B, Patel S, Krause S, Vanko A, Van Hecken A, Dupont P, De Lepeleire I, Rothenberg P, Stoch SA, Cote J, Hagmann WK, Jewell JP, Lin LS, Liu P, Goulet MT, Gottesdiener K, Wagner JA, de Hoon J, Mortelmans L, Fong TM, Hargreaves RJ. 2007. [<sup>18</sup>F]MK-9470, a positron emission tomography (PET) tracer for *in vivo* human PET brain imaging of the cannabinoid-1 receptor. *Proc Natl Acad Sci USA* 104:9800–9805.
- Clark JD, Baldwin RL, Bayne KA, Brown MJ, Gebhart GF, Gonder JC, Gwathmey JK, Keeling ME, Kohn DF, Robb JW, Smith OA, Steggerda J-AD, VandeBergh JL. 1996. Guide for the care and use of laboratory animals. Washington, DC: National Academies Press.
- Darmani NA, Crim JL. 2005. Delta-9-tetrahydrocannabinol differentially suppresses emesis versus enhanced locomotor activity produced by chemically diverse dopamine D<sub>2</sub>/D<sub>3</sub> receptor agonists in the least shrew (*Cryptotis parva*). *Pharmacol Biochem Behav* 80:35–44.
- Devane WA, Dysarz FA, III, Johnson MR, Melvin LS, Howlett AC. 1988. Determination and characterization of a cannabinoid receptor in rat brain. *Mol Pharmacol* 34:605–613.
- Devane WA, Hanus L, Breuer A, Pertwee RG, Stevenson LA, Griffin G, Gibson D, Mandelbaum A, Etinger A, Mechoulam R. 1992. Isolation and structure of a brain constituent that binds to the cannabinoid receptor. *Science* 258:1946–1949.
- Donohue SR, Halldin C, Schou M, Hong J, Phebus L, Chernet E, Hitchcock SA, Gardinier KM, Ruley KM, Krushinski JH, Schaus J, Pike VW. 2008. Radiolabeling of a high affinity cannabinoid subtype-1 receptor inverse agonist, *N*-(4-fluoro-benzyl)-4-(3-(piperidin-1-yl)-indole-1-sulfonyl)benzamide (PipISB), with carbon-11 or fluorine-18. *J Label Compd Radiopharm* 51:146–152.
- Fan H, Ravert HT, Holt DP, Dannals RF, Horti AG. 2006. Synthesis of 1-(2,4-dichlorophenyl)-4-cyano-5-(4-[<sup>14</sup>C]methoxyphenyl)-*N*-(piperidin-1-yl)-1*H*-pyrazole-3-carboxamide ([<sup>14</sup>C]JHU75528) and 1-(2-bromophenyl)-4-cyano-5-(4-[<sup>14</sup>C]methoxyphenyl)-*N*-(piperidin-1-yl)-1*H*-pyrazole-3-carboxamide ([<sup>14</sup>C]JHU75575) as potential radioligands for PET imaging of cerebral cannabinoid receptor. *J Label Compd Radiopharm* 49:1021–1036.
- Gandelman M, Baldwin RM, Zoghbi SS, Zea-Ponce Y, Innis RB. 1994. Evaluation of ultrafiltration for the free fraction determination of SPECT radiotracers: β-CIT, IBF and iomazenil. *J Pharm Sci* 83:1014–1019.
- Glass M, Dragunow M, Faull RL. 1997. Cannabinoid receptors in the human brain: A detailed anatomical and quantitative autoradiographic study in the fetal, neonatal and adult human brain. *Neuroscience* 77:299–318.
- Gong JP, Onaivi ES, Ishiguro H, Liu QR, Tagliaferro PA, Brusco A, Uhl GR. 2006. Cannabinoid CB<sub>2</sub> receptors: Immunohistochemical localization in rat brain. *Brain Res* 1071:10–23.
- Grundy RI. 2002. The therapeutic potential of the cannabinoids in neuroprotection. *Expert Opin Invest Drugs* 11:1365–1374.
- Halford JC. 2006. Obesity drugs in clinical development. *Curr Opin Invest Drugs* 7:312–318.
- Halldin C, Swahn CG, Farde L, Sedvall G. 1995. Radioligand disposition and metabolism. In: Comar D, editor. PET for drug development and evaluation. Dordrecht, Netherlands: Kluwer. p 55–65.
- Halldin C, Gulyas B, Farde L. 2001. PET studies with carbon-11 radioligands in neuropsychopharmacological drug development. *Curr Pharm Des* 7:1907–1929.
- Henningfield JE, Fant RV, Buchhalter AR, Stitzer ML. 2005. Pharmacotherapy for nicotine dependence. *CA Cancer J Clin* 55:281–299.
- Herkenham M, Lynn AB, Little MD, Johnson MR, Melvin LS, De Costa BR, Rice KC. 1990. Cannabinoid receptor localization in brain. *Proc Natl Acad Sci USA* 87:1932–1936.
- Herkenham M, Lynn AB, Johnson MR, Melvin LS, De Costa BR, Rice KC. 1991. Characterization and localization of cannabinoid receptors in rat brain: A quantitative *in vitro* autoradiographic study. *J Neurosci* 11:563–583.
- Horti AG, Fan H, Kuwabara H, Hilton J, Ravert HT, Holt DP, Alexander M, Kumar A, Rahmim A, Scheffel U, Wong DF, Dannals RF. 2006. [<sup>11</sup>C]JHU75528: A radiotracer for PET imaging of CB<sub>1</sub> cannabinoid receptors. *J Nucl Med* 47:1689–1696.
- Izzo AA, Coutts AA. 2005. Cannabinoids and the digestive tract. *Handb Exp Pharmacol* 168:573–598.
- Landsman RS, Burkey TH, Consroe P, Roeske WR, Yamamura HI. 1997. SR141716A is an inverse agonist at the human cannabinoid CB<sub>1</sub> receptor. *Eur J Pharmacol* 334:R1–R2.
- Liu P, Lin LS, Hamill TG, Jewell JP, Lanza TJ, Jr, Gibson RE, Krause SM, Ryan C, Eng W, Sanabria S, Tong X, Wang J, Levsore DA, Owens KA, Fong TM, Shen CP, Lao J, Kumar S, Yin W, Payack JF, Springfield SA, Hargreaves R, Burns HD, Goulet MT, Hagmann WK. 2007. Discovery of *N*-((1*S*,2*S*)-2-(3-cyanophenyl)-3-[4-(2-[<sup>18</sup>F]fluoroethoxy)phenyl]-1-methylpropyl)-2-methyl-2-[(5-methylpyridin-2-yl)oxy]propanamide, a cannabinoid-1 receptor positron emission tomography tracer suitable for clinical use. *J Med Chem* 50:3427–3430.
- Lynn AB, Herkenham M. 1994. Localization of cannabinoid receptors and nonsaturable high-density cannabinoid binding-sites in peripheral-tissues of the rat: Implications for receptor-mediated immune modulation by cannabinoids. *J Pharmacol Exp Ther* 268:1612–1623.
- Mechoulam R, Ben-Shabat S, Hanus L, Ligumsky M, Kaminski NE, Schatz AR, Gopher A, Almog S, Martin BR, Compton DR, Pertwee RG, Griffin G, Bayewitch M, Barg J, Vogel Z. 1995. Identification of an endogenous 2-monoglyceride, present in canine gut, that binds to cannabinoid receptors. *Biochem Pharmacol* 50:83–90.
- Meschler JP, Kraichely DM, Wilken GH, Howlett AC. 2000. Inverse agonist properties of *N*-(piperidin-1-yl)-5-(4-chlorophenyl)-1-(2,4-dichlorophenyl)-4-methyl-1*H*-pyrazole-3-carboxamide HCl (SR141716A) and 1-(2-chlorophenyl)-4-cyano-5-(4-methoxyphenyl)-1*H*-pyrazole-3-carboxylic acid phenylamide (CP-272871) for the CB<sub>1</sub> cannabinoid receptor. *Biochem Pharmacol* 60:1315–1323.
- Mozley PD. 2005. Weaving single photon emission tomography into new drug development. *Mol Imaging Biol* 7:30–36.
- Munro S, Thomas KL, Abushaar M. 1993. Molecular characterization of a peripheral receptor for cannabinoids. *Nature* 365:61–65.
- Pryce G, Ahmed Z, Hankey DJ, Jackson SJ, Croxford JL, Pocock JM, Ledent C, Petzold A, Thompson AJ, Giovannoni G, Cuzner ML, Baker D. 2003. Cannabinoids inhibit neurodegeneration in models of multiple sclerosis. *Brain* 126:2191–2202.
- Rinaldi-Carmona M, Barth F, Héaulme M, Shire D, Calandra B, Congy C, Martinez S, Maruani J, Néliat G, Caput D, Ferrara P, Soubrie P, Breliere JC, Le Fur G. 1994. SR141716A, a potent and selective antagonist of the brain cannabinoid receptor. *FEBS Lett* 350:240–244.
- Roland PE, Graufelds CJ, Wählin J, Ingelman L, Andersson M, Ledberg A, Pedersen J, Akerman S, Dabringhaus A, Zilles K. 1994. Human brain atlas: For high-resolution functional and anatomical mapping. *Hum Brain Mapp* 1:173–184.
- Sugiura T, Kondo S, Sukagawa A, Nakane S, Shinoda A, Itoh K, Yamashita A, Waku K. 1995. 2-Arachidonoylglycerol: A possible endogenous cannabinoid receptor ligand in brain. *Biochem Biophys Res Commun* 215:89–97.
- Wienhard K, Dahlbom M, Eriksson L, Michel C, Bruckbauer T, Pietrzyk U, Heiss WD. 1994. The ECAT EXACT HR: Performance of a new high resolution positron scanner. *J Comput Assist Tomogr* 18:110–118.
- Yasuno F, Brown AK, Zoghbi SS, Krushinski JH, Chernet E, Tauscher J, Schaus JM, Phebus LA, Chesterfield AK, Felder CC, Gladding RL, Hong J, Halldin C, Pike VW, Innis RB. 2008. The PET radioligand [<sup>14</sup>C]MePPEP binds reversibly and with high specific signal to cannabinoid CB<sub>1</sub> receptors in nonhuman primate brain. *Neuropsychopharmacology* 33:259–269.
- Zoghbi SS, Shetty HU, Ichise M, Fujita M, Imaizumi M, Liow JS, Shah J, Musachio JL, Pike VW, Innis RB. 2006. PET imaging of the dopamine transporter with [<sup>18</sup>F]-FECNT: A polar radiometabolite confounds brain radioligand measurements. *J Nucl Med* 47:520–527.